Liver X receptor β regulates the development of the dentate gyrus and autistic-like behavior in the mouse

Yulong Cai[a,b,1], Xiaotong Tang[b,1], Xi Chen[c], Xin Li[a], Ying Wang[a], Xiaohang Bao[d], Lian Wang[a], Dayu Sun[a], Jinghui Zhao[a], Yan Xing[a], Margaret Warner[e], Haiwei Xu[f], Jan-Åke Gustafsson[e,g,2], and Xiaotang Fan[a,2]

[a]Department of Developmental Neuropsychology, School of Psychology, Third Military Medical University, 400038 Chongqing, China; [b]Department of Histology and Embryology, Third Military Medical University, 400038 Chongqing, China; [c]School of Medicine, Nankai University, 300071 Tianjin, China; [d]Department of Anesthesiology, Xinqiao Hospital, Third Military Medical University, 400038 Chongqing, China; [e]Center for Nuclear Receptors and Cell Signaling, University of Houston, Houston, TX 77054; [f]Southwest Eye Hospital, Southwest Hospital, Third Military Medical University, 400038 Chongqing, China; and [g]Center for Innovative Medicine, Department of Biosciences and Nutrition, Karolinska Institute, 141 86 Novum, Sweden

Contributed by Jan-Åke Gustafsson, February 6, 2018 (sent for review January 5, 2018; reviewed by Luis M. Garcia-Segura and Jin Peng)

The dentate gyrus (DG) of the hippocampus is a laminated brain region in which neurogenesis begins during early embryonic development and continues until adulthood. Recent studies have implicated that defects in the neurogenesis of the DG seem to be involved in the genesis of autism spectrum disorders (ASD)-like behaviors. Liver X receptor β (LXRβ) has recently emerged as an important transcription factor involved in the development of laminated CNS structures, but little is known about its role in the development of the DG. Here, we show that deletion of the LXRβ in mice causes hypoplasia in the DG, including abnormalities in the formation of progenitor cells and granule cell differentiation. We also found that expression of Notch1, a central mediator of progenitor cell self-renewal, is reduced in LXRβ-null mice. In addition, LXRβ deletion in mice results in autistic-like behaviors, including abnormal social interaction and repetitive behavior. These data reveal a central role for LXRβ in orchestrating the timely differentiation of neural progenitor cells within the DG, thereby providing a likely explanation for its association with the genesis of autism-related behaviors in LXRβ-deficient mice.

LXRβ | dentate gyrus | development | progenitor cells | autism

The dentate gyrus (DG) is involved in higher brain functions, such as learning and memory processing (1). The subgranular zone (SGZ) of the hippocampal DG is endowed with a pool of neural precursor cells (NPCs) that can divide and produce granule cells through postnatal life (2). Autism spectrum disorders (ASD) represent a neurodevelopmental disorder characterized by impairments in social communication and interactions as well as restricted and repetitive behaviors. Defective DG formation and dysregulated neurogenesis have been observed in patients with ASD (3, 4). Recent studies have suggested that certain strategies ameliorated ASD-like behaviors as well as enhanced DG neurogenesis (5). However, the molecular reasons for these changes in relation to ASD remain largely elusive.

The formation of the DG is a complex process involving cell proliferation, migration, and differentiation (6, 7). Studies have indicated that radial glial cells (RGCs) are critical for the normal development of the lamination of the DG, acting as neurogenic progenitors producing neurons and providing the scaffold for guidance of the migration of newborn neurons and progenitor cells (8). RGCs still reside in the adult SGZ and contribute to hippocampal neurogenesis. Meanwhile, a large body of evidence has indicated that molecules that regulate the development of RGCs have an essential function in DG development (9). Considering the important roles of RGCs in DG development, understanding the functions of RGCs in DG development may help elucidate the mechanisms that regulate hippocampal neurogenesis.

The liver X receptors (LXR), LXRα and LXRβ, are ligand-activated transcription factors (10). The LXRα is primarily expressed in adipose tissue, the liver, and the intestine, whereas the LXRβ is broadly expressed in the developing and adult rodent brain (11). Our previous studies demonstrated that LXRβ is essential for layering in the neocortex and cerebellum, via regulation of RGC development (12–14). In the neocortex, loss of LXRβ results in developmental impairment of the vertical processes of RGCs and, thus, causes delayed migration of later-born neurons (12). In the cerebellum, activation of LXR prevented premature differentiation of Bergmann glia and promoted granule neuron migration and development of Purkinje cell dendrites (13, 14). Most recently, we showed that the LXRβ affects white matter development and CNS myelination by regulating the commitment of RGCs to differentiation into oligodendrocyte progenitor cells or astrocytes (15). Although the LXRβ has been implicated in the development of laminated CNS structures through modulation of RGC development, little is known about its role in DG development.

In the present study, we found that the LXRβ plays a central role in orchestrating the timely differentiation of NPCs within the developing DG, and in doing so determines precursor proliferation, differentiation, and neurogenesis. We show that LXRβ deletion in mice perturbs RGC development via down-regulation of expression of Notch1 signaling and causes autism-like behaviors. These findings provide a causal role for the loss of the LXRβ in the genesis of autism-related behaviors.

Results

Formation of the Transient Neurogenic Zone Requires LXRβ Signaling. Formation of the DG starts during late embryogenesis when dentate

Significance

Defects in the neurogenesis of the dentate gyrus (DG) seem to be involved in the genesis of autism spectrum disorders (ASD)-like behaviors. Our study reveals that deletion of the Liver X receptor β (LXRβ) in mice causes hypoplasia in the DG, including abnormalities in the formation of progenitor cells and reduced neurogenesis. Behavioral analysis of LXRβ-deficient mice showed autistic-like behaviors, including social interaction deficits and repetitive behavior. These findings provide evidence that early changes in DG neurogenesis is possibly associated with the genesis of autism-related behaviors in LXRβ-deficient mice.

Author contributions: M.W., J.-Å.G., and X.F. designed research; Y.C., X.T., X.C., X.L., Y.W., X.B., L.W., D.S., J.Z., and Y.X. performed research; Y.C., X.T., M.W., H.X., J.-Å.G., and X.F. analyzed data; and M.W., J.-Å.G., and X.F. wrote the paper.

Reviewers: L.M.G.-S., Instituto Cajal; and J.P., Emory University.

The authors declare no conflict of interest.

[1]Y.C. and X.T. contributed equally to this work.

[2]To whom correspondence may be addressed. Email: jgustafsson@uh.edu or fanxiaotang2005@163.com.

This article contains supporting information online at www.pnas.org/lookup/suppl/doi:10.1073/pnas.1800184115/-/DCSupplemental.

Published online March 5, 2018.

precursors migrate from the neuroepithelium (16, 17). Using a specific antibody, we observed the dynamic expression of the LXRβ during DG development (*SI Appendix*, Fig. S1), suggesting its role in DG formation. Brain lipid binding protein (BLBP) labeled RGCs in the forming dentate (9). At embryonic day (E)15.5, there was a robust stream of BLBP$^+$ cells in the fimbriodentate junction (FDJ) of wild-type (WT) mice (arrow in Fig. 1*A*), but the area occupied by BLBP$^+$ cells was much smaller in the LXRβ mutants (arrow in Fig. 1*B*). BLBP$^+$ cell bodies were clearly identified in the FDJ, and some of them had already reached the hippocampal fissure (HF); the transhilar radial glial scaffold was clearly labeled by BLBP in the forming dentate at E18.5 (Fig. 1*C*). In LXRβ knockout (KO) mice, there were fewer BLBP$^+$-labeled somas in the HF and hilus, and a subset of transhilar glial fibers labeled by BLBP was reduced in the mutants (Fig. 1*D*). By postnatal day (P)2, GFAP$^+$ processes were more enriched in the HF and the transient subpial neurogenic zone (SPZ) in the controls (Fig. 1 *E* and *G*) than in the mutants (Fig. 1 *F* and *H*). Meanwhile, Nestin$^+$ cells and processes appeared to spread toward the hilus from the SPZ in control mice (Fig. 1*I*); both were decreased in LXRβ KO mice (Fig. 1*J*). As the granule cell layer (GCL) formed from SPZ, BLBP$^+$ cell bodies became localized in the GCL in control mice, and a few cells were observed migrating along the transhilar radial glial scaffold through the hilus (Fig. 1*K*). However, in LXRβ KO mice, most of the BLBP$^+$ cell bodies remained in the SPZ. In addition, BLBP$^+$-labeled cells were randomly oriented across the hilus, failing to obtain the characteristic radial orientation of the transhilar radial glial scaffold (Fig. 1*L*). In the developing DG, the T-box transcription factor (*Tbr2*) is specifically expressed in intermediate progenitor cells (IPCs) and critical for DG neurogenesis (18). At P2 in control mice, most Tbr2$^+$ IPCs were restricted to the SPZ (Fig. 1*M*), a few Tbr2$^+$ cells were also present in the GCL (Fig. 1*O*). In contrast, in LXRβ KO mice, at P2, there were fewer Tbr2$^+$ cells in the SPZ and GCL (Fig. 1 *N*, *P*, and *U*). At the end of the first postnatal week, the transient SPZ is essentially depleted and replaced by marginal zone (MZ) (19). The condensed Tbr2$^+$ cell population in the control DGs was separated into two bands, one in the MZ and another in the SGZ. The Tbr2$^+$ IPCs in the MZ were reduced and largely found in the SGZ (Fig. 1*Q*). There were fewer Tbr2$^+$ IPCs in mutants, and the cell band in the SGZ was absent in mutant DGs (Fig. 1*R*). Prox1 was selectively expressed in dentate granule cells and their progenitors (20). We found that there were significantly fewer Prox1$^+$ cells in the developing DG of LXRβ KO mice at P2 (Fig. 1 *T* and *V*) than in control littermates (Fig. 1*S*). Accordingly, we can infer that LXRβ is involved in the formation of the transient neurogenic zone.

Loss of LXRβ Reduces Neuronal Progenitor Cell Proliferation. To identify proliferating cells within the DG, we performed short-pulse labeling with BrdU. Examining proliferating cells of the postnatal DG revealed a greatly reduced number of BrdU$^+$-positive cells at P2 by 24% ($P < 0.01$) in the mutant DGs (Fig. 2 *A*, *B*, and *Q*). At

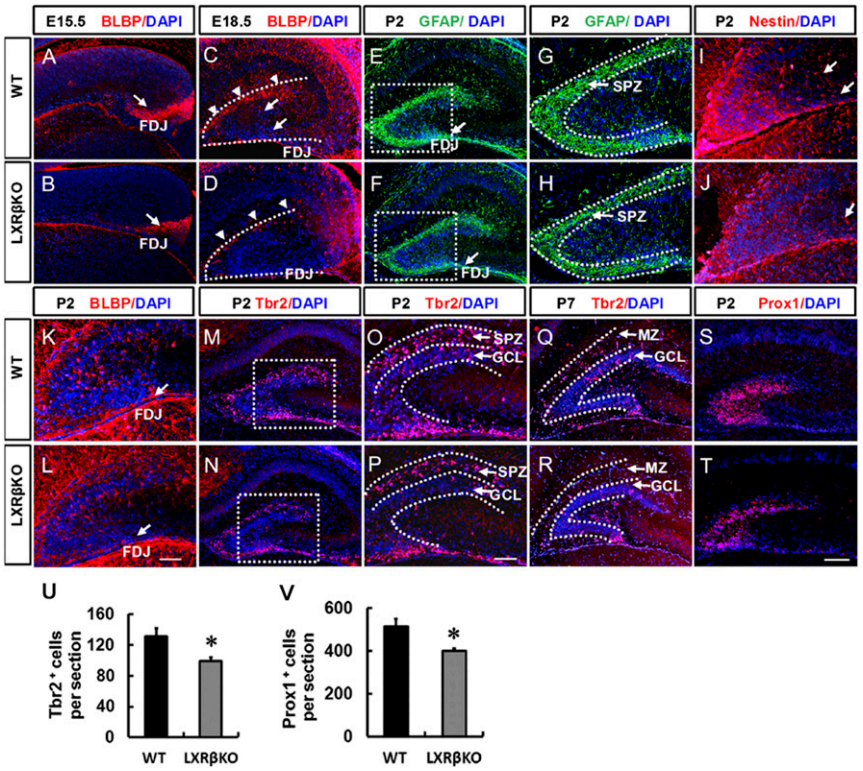

Fig. 1. Defective subpial neurogenic zone, abnormal radial glial scaffolding, and decreased granule cell production in LXRβ-null mice. At E15.5 (*A* and *B*), BLBP$^+$ RGCs formed a new neurogenic zone in the subpial region of the FDJ. Loss of LXRβ decreased BLBP-positive cells in the FDJ. Arrows in *A* and *B* indicate the FDJ. At E18.5 (*C* and *D*), BLBP$^+$ RGCs crossed the hilus and formed the hippocampal fissure, and loss of LXRβ decreased BLBP-positive cells in the hippocampal fissure. Arrowheads in *C* and *D* indicate hippocampal fissure; arrows in *C* indicate transhilar radial glial scaffold. At P2, GFAP$^+$ processes were more enriched in the transient SPZ of WT animals (*E* and *G*) compared with the mutants (*F* and *H*). Arrows in *E* and *F* indicate FDJ. The SGZ started to take shape. BLBP-positive (*K* and *L*) and Nestin-positive (*I* and *J*) cells began to seed the nascent SGZ. Loss of LXRβ decreased BLBP-positive and Nestin-positive cells. Arrows in *I* and *J* indicate the transhilar radial glial scaffold, arrows in *K* and *L* indicate the FDJ. Tbr2$^+$ cells were mainly localized in the SPZ of control animals (*M* and *O*), which was decreased in the mutant DGs (*N* and *P*) at P2. By P7, as most of the Tbr2$^+$ cells were localized in the GCL, fewer cells were observed in the GCL in the mutant DGs (*R*) compared with WT controls (*Q*). At P2, Prox1$^+$ granule cells were decreased in the DG of mutants (*T*) compared with WT controls (*S*). Quantitative analysis of the number of Tbr2$^+$ (*U*) and Prox1$^+$ (*V*) cells in the DG ($n = 3$, $^*P < 0.05$, Student's *t* test) (*G*, *H*, *O*, and *P*). Images are higher-power views of the boxed areas in *E*, *F*, *M*, and *N*. Data are presented as mean ± SEM. (Scale bars: *T* for *A*–*F*, *M*, *N*, and *Q*–*T*, 100 μm; *L* for *G*–*L*, *O*, and *P*, 50 μm.)

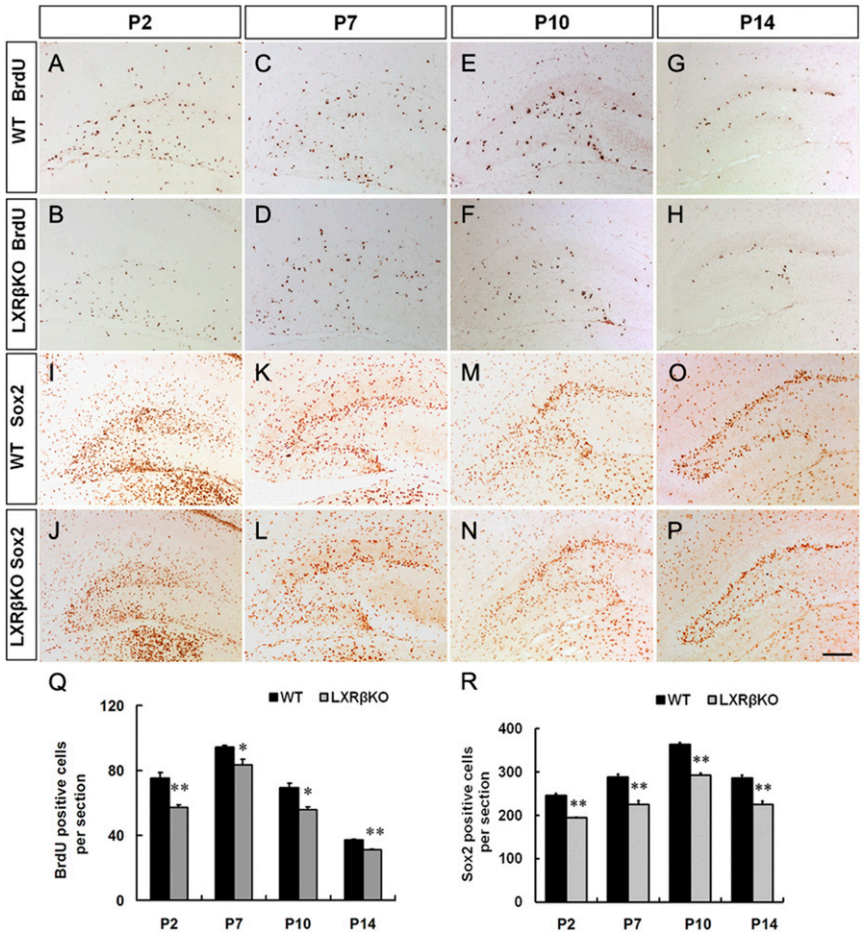

Fig. 2. Loss of LXRβ decreased BrdU-labeled nuclei and Sox2 expression in the DG from P2 to P14. (*A–H*) Representative images of BrdU-immunolabeled coronal sections of the DG of mice at P2 (*A* and *B*), P7 (*C* and *D*), P10 (*E* and *F*), and P14 (*G* and *H*). (*I–P*) Representative images of Sox2-immunolabeled coronal sections of the DG of mice at P2 (*I* and *J*), P7 (*K* and *L*), P10 (*M* and *N*), and P14 (*O* and *P*). (*Q*) Quantitative analysis of the number of BrdU-labeled cells in the hippocampal DG. (*R*) Quantitative analysis of the number of Sox2-labeled cells in the hippocampal DG. Data are presented as the mean cells in DG per section ± SEM, $n = 3$. $^{*}P < 0.05$, $^{**}P < 0.01$, versus WT controls; Student's *t* test. (Scale bar: 100 μm.)

P7, $BrdU^{+}$ cells were mainly localized in the GCL in control DGs (Fig. 2*C*), significantly decreased by 11.5% in the mutant DGs ($P < 0.05$) (Fig. 2 *D* and *Q*). At P10 (Fig. 2 *E* and *F*) and P14 (Fig. 2 *G* and *H*), when the majority of proliferating progenitor cells were located in the newly developed SGZ, BrdU-positive cells in the DG were decreased by 19.9% at P10 ($P < 0.05$) (Fig. 2*Q*) and by 16.3% at P14 ($P < 0.01$) (Fig. 2*Q*) in the mutant mice. Meanwhile, we observed that Sox2-expressing progenitors in the mutant DG were significantly decreased by 20.9% at P2 (Fig. 2 *I*, *J*, and *R*), 22% at P7 (Fig. 2 *K*, *L*, and *R*), 19.5% at P10 (Fig. 2 *M*, *N*, and *R*), and 21.5% at P14 (Fig. 2 *O*, *P*, and *R*) compared with control DGs. To investigate the effect of T0901317, the LXR agonist which has been used to study the function of endogenous LXR, on the proliferation of RGC cell line L2.3, we measured the Ki67 staining intensity. On days 2 and 3, 1 μM T0901317 exposure significantly increased the Ki67 incorporation ratio compared with the control group (*SI Appendix*, Fig. S2). However, 10 μM T0901317 decreased the ratio of Ki67-positive cells after a 3-d treatment (*SI Appendix*, Fig. S2). The cell cycle analysis supported the conclusion that 1 μM T0901317 increased the proliferation of L2.3 cells, whereas the 10 μM dose had an inhibitory impact, which was consistent with the Ki67 staining results (*SI Appendix*, Fig. S3).

We next examined the effects of LXRβ deficiency on the migration of dentate precursors. To trace the migrating dentate precursors, we injected BrdU at E15.5 and performed analysis at E18.5. At the rostral level, the migration of dentate precursors to the DG was delayed by loss of LXRβ (*SI Appendix*, Fig. S4 *A–F*). We also performed analysis of BrdU staining in the mice at P7 after injection with BrdU at P2. A substantial decrease in the ratio of BrdU-positive cells was observed in the GCL of LXRβ KO mice (*SI Appendix*, Fig. S4 *I* and *J*) compared with control mice [(*SI Appendix*, Fig. S4 *G* and *H*) at both rostral (88.6% of the control, $P < 0.05$) (*SI Appendix*, Fig. S4 *G*, *I*, and *K*) and caudal level (81.3% of the control, $P < 0.01$) (*SI Appendix*, Fig. S2 *H*, *J*, and *L*)].

LXRβ Loss Delays Secondary RGC Development Through the Notch1 Signaling Pathway. The secondary radial glial scaffold initially develops in the first postnatal week, whose processes traverse the forming GCL and is fully developed around P10 to P14 (21). The secondary radial glial scaffold has been implicated in DG formation (22, 23). Possibly, the deletion of LXRβ disturbs the development of the secondary radial glial scaffold. BLBP immunoreactivity is largely confined to the soma and nuclei of secondary radial cells within the SGZ. The unbranched radial processes extending toward the molecular layer can be visualized by GFAP immunoreactivity. In DG mutants, the pool of NPCs in the SGZ was significantly decreased compared with control DGs, as measured by their radial glial morphology with expression of both BLBP and GFAP at P7 (80.9% of the control, $P < 0.01$; Fig. 3 *A–D* and *Q*) and P14 (79.5% of the control, $P < 0.05$; Fig. 3 *E–H* and *Q*).

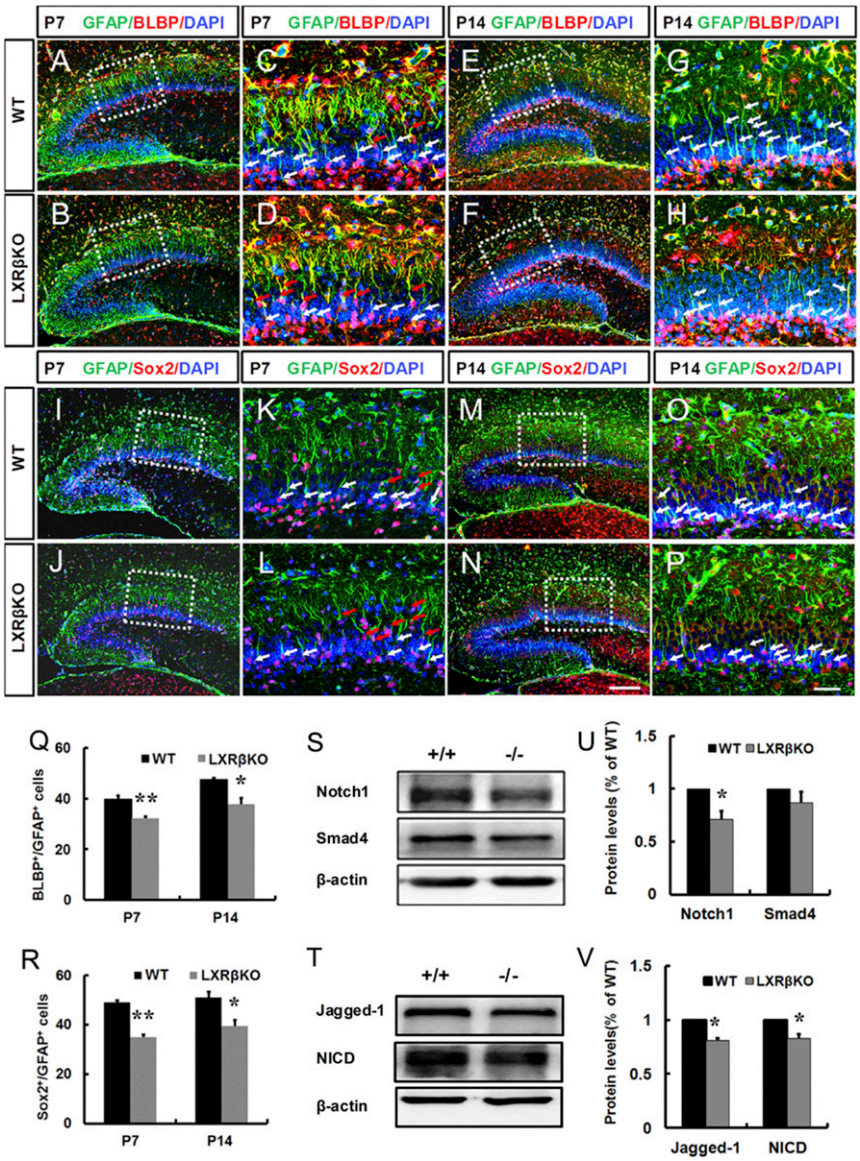

Fig. 3. Loss of LXRβ decreased secondary RGCs in the SGZ of mice at P7 and P14. (*A–H*) Representative images of BLBP and GFAP double-positive RGCs in the DG of mice at P7 (*A–D*) and P14 (*E–H*). (*C*, *D*, *G*, and *H*) Images are higher-power views of the boxed areas in *A*, *B*, *E*, and *F*. Arrows in *C*, *D*, *G*, and *H* indicate $BLBP^+/GFAP^+$ double-staining cells in the SGZ (White) and GCL (Red). (*I–P*) Representative images of $GFAP^+$ and $Sox2^+$ double-positive RGCs in the DG of mice at P7 (*I–L*) and P14 (*M–P*). (*K*, *L*, *O*, and *P*) Images are higher-power views of the boxed areas in *I*, *J*, *M*, and *N*. Arrows in *K*, *L*, *O*, and *P* indicate $Sox2^+/GFAP^+$ double-staining cells in the SGZ (white) and GCL (red). Quantitative analysis of the number of $BLBP^+/GFAP^+$ (*Q*) and $GFAP^+/Sox2^+$ (*R*) double-stained cells in the SGZ ($n = 3$, $^*P < 0.05$; $^{**}P < 0.01$, Student's *t* test). (Scale bars: *N* for *A*, *B*, *E*, *F*, *I*, *J*, *M*, and *N*, 100 μm; *P* for *C*, *D*, *G*, *H*, *K*, *L*, *O*, and *P*, 50 μm.) (*S–V*) Western blot analysis of the Notch1 signaling pathway (Notch1, NICD, Jagged1) and Smad4 in P7 WT and LXRβ KO hippocampus. (*S*) Representative immunoblots of Notch1 and Smad4. (*U*) Graph representing the densitometric analysis of Notch1 and Smad4. ($n = 3$, $^*P < 0.05$, Student's *t* test). (*T*) Representative immunoblots of Jagged1 and NICD. (*V*) Graph representing the densitometric analysis of Jagged1 and NICD ($n = 3$, $^*P < 0.05$, Student's *t* test). Data are presented as mean ± SEM.

Similarly, we further confirmed that $Sox2^+/GFAP^+$ double-stained RGC cells in the SGZ were also decreased by loss of LXRβ at P7 (71.5% of the control, $P < 0.01$; Fig. 3 *I–L* and *R*) and P14 (77.3% of the control, $P < 0.05$; Fig. 3 *M–P* and *R*). However, we also noticed that both $BLBP^+/GFAP^+$ (red arrows in Fig. 3 *C* and *D*) and $GFAP^+/Sox2^+$ (red arrows in Fig. 3 *K* and *L*) double-stained RGCs retained in the GCL were increased by loss of LXRβ.

Notch1 signaling and Smad4 activating pathways contribute to RGC development in the developing DG (24–26). After standardization to actin, the mean level of Notch1 in the hippocampus from LXRβ KO mice was significantly decreased compared with WT littermates (Fig. 3 *S* and *U*). However, there was no significant alteration in the Smad4 level in LXRβ KO mice, compared with those of WT animals (Fig. 3 *S* and *U*). Moreover, Notch1 intracellular domain (NICD), as Notch1 cleavage has been indicated in early postnatal DG development (24), was measured. Analysis of hippocampal homogenates by immunoblot revealed a 17% reduction in NICD levels in LXRβ KO mice (Fig. 3 *T* and *V*). Thus, LXRβ deficiency reduces Notch1 activation or leads to a destabilization of NICD. The observed reduction in Notch1 activation could result from a reduced expression of Notch1 ligands. Therefore, we measured the expression level of the Notch1 ligand, Jagged1. Western blot analysis showed that the mean level of Jagged1 in the hippocampus was significantly reduced in

LXRβ KO mice compared with WT animals (Fig. 3 *T* and *V*). In addition, our data showed that LXRβ loss decreased the levels of Hes1 and BLBP, downstream effectors of Notch1 (*SI Appendix*, Fig. S5), which might be involved in the reduction of secondary RGCs during early postnatal DG development.

LXRβ Ablation Impairs Neuronal Differentiation. To determine the role of LXRβ in the regulation of granule cell differentiation, we evaluated the expression of stage-specific markers in control and mutant animals. At P7, most of Calretinin-labeled immature granule cells were localized in the GCL of control mice (Fig. 4*A*) and was decreased by loss of LXRβ (Fig. 4*B*). Calbindin (CB) expression in the GCL of the DG indicates functional maturity of the hippocampal formation (27). At P7, a general distribution pattern of CB was shown in the dorsal blade of the GCL, and a few CB^+ cells were generated in the ventral blade (Fig. 4*C*). Loss of LXRβ decreased CB^+ cells in the dorsal blade of the GCL, and fewer CB^+ cells were detected in the ventral blade (Fig. 4 *D* and *K*).

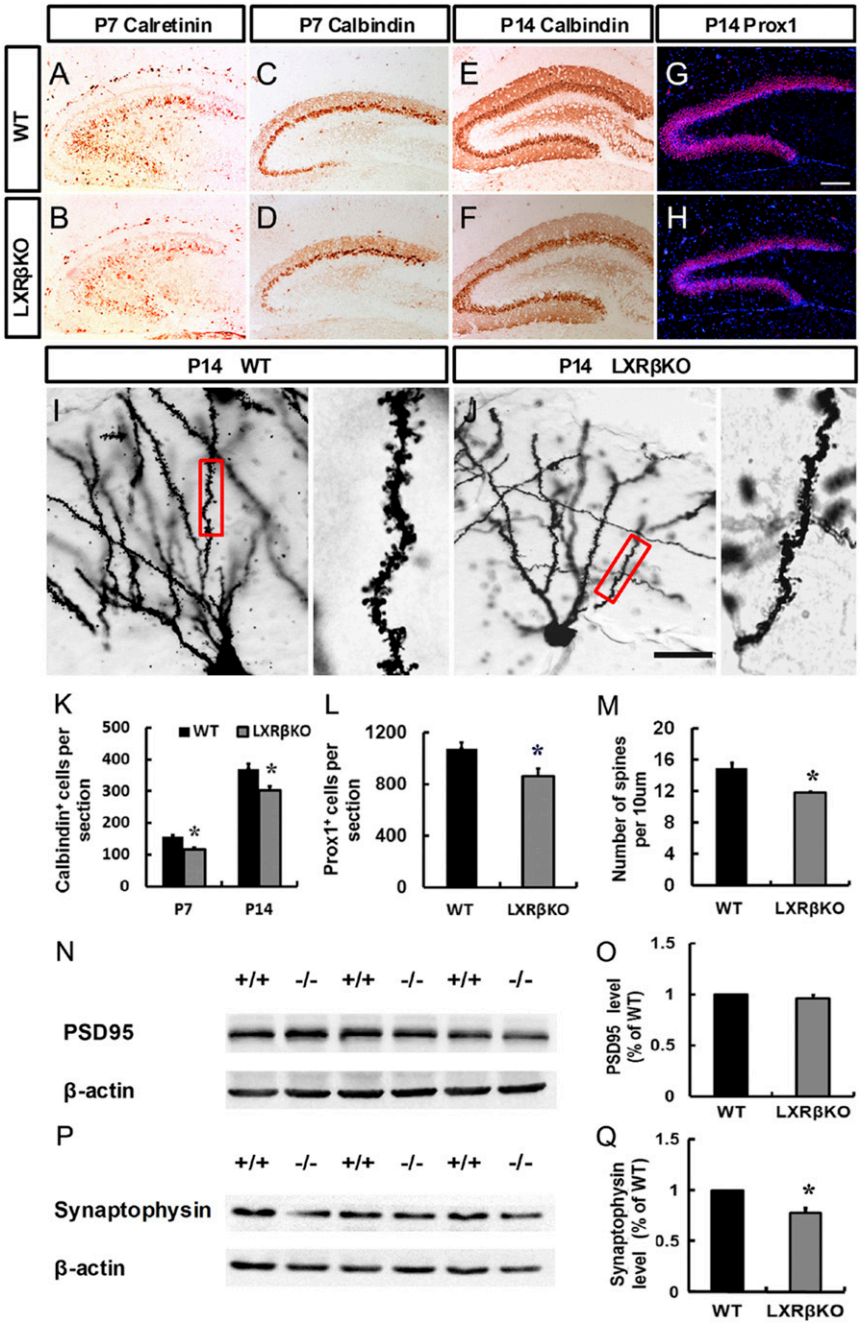

Fig. 4. Loss of LXRβ disrupted dentate granule cell differentiation. (*A* and *B*) Immunohistological analysis of calretinin expression in the DG of control (*A*) and mutant animals (*B*) at P7. (*C*–*F*) Immunohistological analysis of calbindin expression in the DG of control (*C* and *E*) and mutant animals (*D* and *F*) at P7 (*C* and *D*) and P14 (*E* and *F*). (*G* and *H*) Immunohistological analysis of Prox1 expression in the DG of control (*G*) and mutant animals (*H*) at P14. (Scale bar: *G* for *A*–*H*, 100 μm; *J* for *I* and *J*, 25 μm.) (*I* and *J*) Golgi stained dendritic impregnated control and LXRβ mutant hippocampi. Statistical analysis of calbindin-positive (*K*) and Prox1-positive (*L*) cells. (*M*) Statistical analysis of dendritic spine numbers of control and LXRβ mutants at P14. Western blot analysis showed a marked decrease in Synaptophysin (*P* and *Q*) in the hippocampal lysates from LXRβKO mice compared with WT at P14. In contrast, no alteration in PSD95 (*N* and *O*) level in the hippocampus was detected between WT and LXRβ KO mice. Data are presented as mean ± SEM, $n = 3$, $^*P < 0.05$, Student's *t* test.

At P14, CB^+ cells (Fig. 4 *E*, *F*, and *K*) and $Prox1^+$ cells (Fig. 4 *G*, *H*, and *L*) were significantly decreased by depletion of LXRβ. BrdU was administered at P5 and P6; brains were harvested at P14 to study the role of LXRβ in the neuronal differentiation. LXRβ deletion decreased the ratio of $BrdU^+/Prox1^+$ double labeled neurons among the BrdU-positive cells (*SI Appendix*, Fig. S6 *A*, *B*, and *E*). However, the ratio of BrdU-labeled astrocytes in the total number of BrdU-labeled cells was increased in mutants (*SI Appendix*, Fig. S6 *C*, *D*, and *F*).

To investigate the dendrite morphology of granule neurons of the DG in LXRβ KO mice at P14, we performed Golgi staining. We found loss of LXRβ induced a significant reduction in the density of dendritic spines of the DG granule neurons (Fig. 4 *I*, *J*, and *M*). Thus, LXRβ deficiency causes alterations in the structure of hippocampal neurons. Synaptic vesicle protein, synaptophysin, is involved in synaptic vesicle exo-endocytosis and synapse formation (28). We found LXRβ KO mice at P14 had lower synaptophysin expression in the hippocampus than had age-matched WT mice (Fig. 4 *P* and *Q*). However, there was no significant change in PSD-95 of the mutant hippocampus (Fig. 4 *N* and *O*). We also examined the role of LXRβ in adult hippocampus neurogenesis by analyzing hippocampal sections 2 h following the last BrdU injection. The LXRβ KO SGZ contained fewer BrdU-positive cells (Fig. 5 *D*–*F*) and DCX-positive neuroblasts (Fig. 5 *A*–*C*). Analysis of differentiation of L2.3 cells revealed that in the presence of 1 μM and 10 μM T0901317, the ratio of $Tuj1^+/BrdU^+$ double-stained cells increased significantly (*SI Appendix*, Fig. S7 *A*, *B*, and *E*), while the ratio of $GFAP^+/BrdU^+$ double-stained cells decreased (*SI Appendix*, Fig. S7 *C*, *D*, and *F*). These data suggest decreased neurogenesis in the DG following LXRβ inactivation.

LXRβ Deletion Results in ASD-Like Behaviors in Mice. Recent studies have indicated that the integrity of the DG is involved in the novel object recognition task (29). In the novel object recognition (NOR) and novel location recognition (NLR) task, there were no significant differences in the discrimination index between the control and the LXRβ KO mice ($P > 0.05$) (Fig. 6 *A* and *B*). We further evaluated the spatial learning and memory in the Morris water maze. There was no significant difference in escape latency between the WT and LXRβ KO mice during training ($P > 0.05$; Fig. 6*E*). The reversal task is used to assess behavioral flexibility. We found that LXRβ KO mice showed impairment in learning the new location of the platform in the reversal task on the Morris water maze (Fig. 6*G*). This indicates that LXRβ deletion in mice mainly reduced cognitive flexibility. Probe trials were performed the day after the last training trial and reversal training; we found that WT and KO animals performed similarly in the probe test (Fig. 6 *F* and *H*). The hippocampus is required for social memory, perhaps because this structure is involved in integrating the complex stimuli necessary for the recognition process (30, 31). We also performed a three-chamber social interaction test in adults. WT mice were more interested in a novel mouse than a novel inanimate object, but LXRβ KO mice had decreased sociability compared with the WT controls (Fig. 6 *I* and *J*). Following this social approach test, we assessed social recognition by testing the mouse's ability to distinguish between a familiar mouse and a new unfamiliar one. WT mice showed a clear preference for the compartment containing the unfamiliar mouse. Remarkably, LXRβ KO mice failed to discriminate between the familiar and unfamiliar mouse (Fig. 6 *K* and *L*). Furthermore, we examined nest building behavior, which is relevant to home-cage social behaviors and dependent on an intact hippocampus (32). LXRβ KO mice were also significantly impaired in this task (Fig. 6*D*). These data indicate that LXRβ

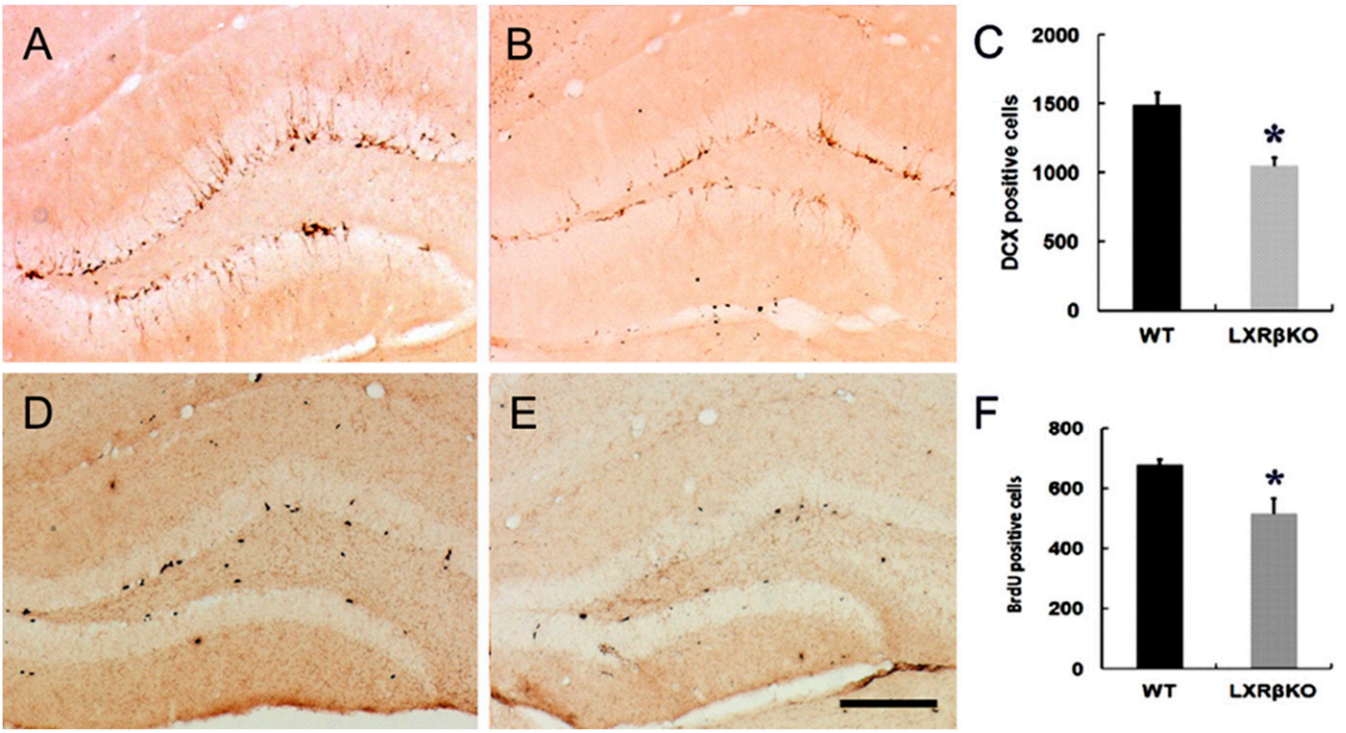

Fig. 5. Loss of LXRβ inhibited adult hippocampus neurogenesis. (*A* and *B*) DCX immunostaining showed normal numbers of hippocampal immature neurons in WT mice while DCX-positive cells were decreased in LXRβKO mice. (*D* and *E*) Loss of LXRβ decreased BrdU-positive cells in the DG (*E*) compared with WT controls (*D*). (*C* and *F*) Statistical analysis of DCX-positive (*C*) and BrdU-positive (*F*) cells. Data are presented as mean ± SEM, $n = 3$, $^*P < 0.05$, Student's *t* test. (Scale bar: 100 μm.)

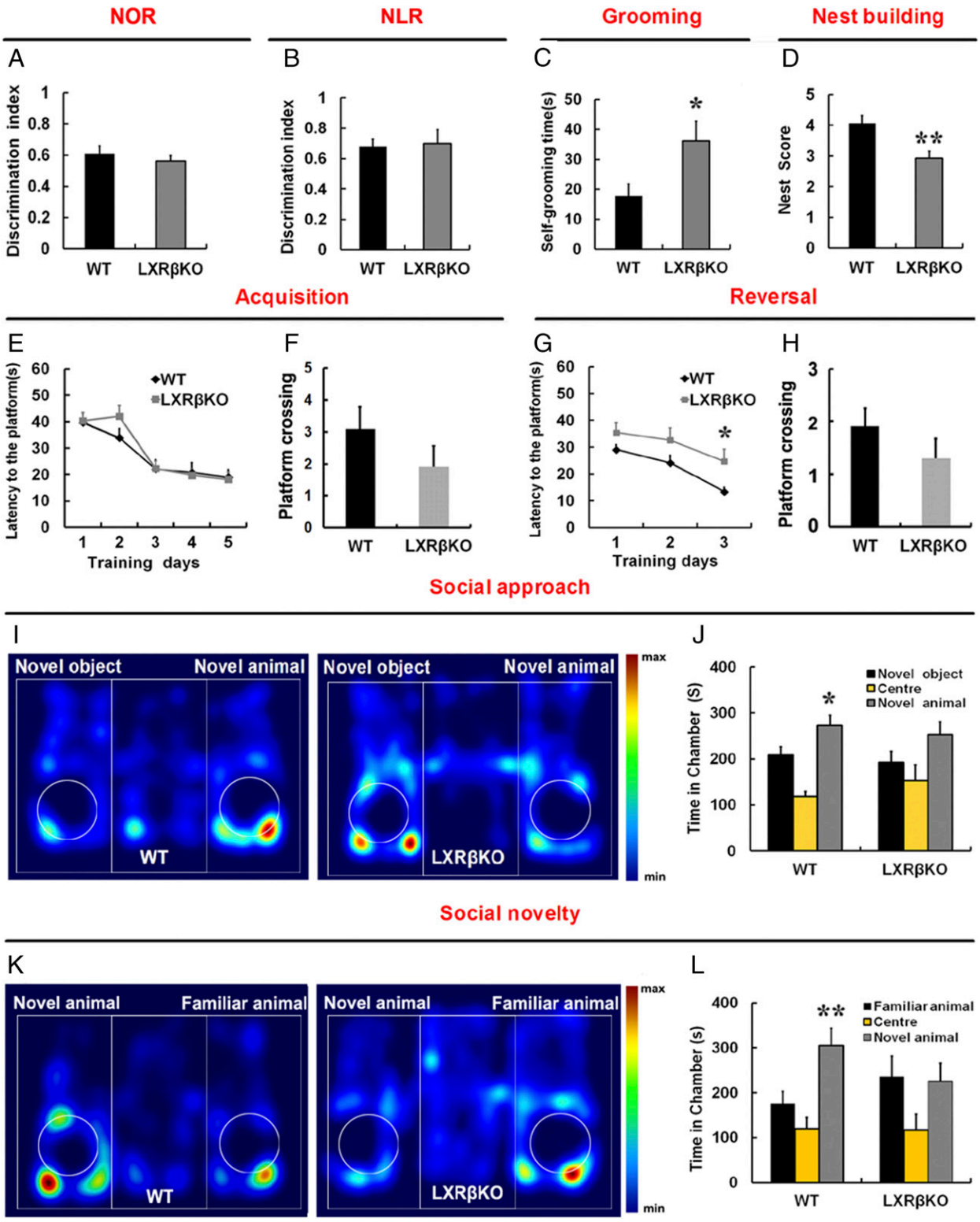

Fig. 6. Loss of LXRβ induced impaired social interaction, increased self-grooming and deficits in cognitive flexibility. (*A*) The discrimination index shows that there is no difference between WT and LXRβ KO mice in the novel object recognition task ($n = 8$, Student's *t* test). (*B*) Discrimination index showed normal preference for the object placed in a new location ($n = 8$, Student's *t* test). (*C*) Time spent grooming over a 10-min period ($n = 9$, $^{*}P < 0.05$, Student's *t* test). (*D*) LXRβKO mice have impaired nest building abilities ($n = 7$, $^{**}P < 0.01$, Student's *t* test). (*E*) In the Morris water maze, LXRβ KO mice displayed normal acquisition ($n = 11$ WT, 10 LXRβ KO, $P > 0.05$, two-way ANOVA, Bonferroni multiple comparison test). (*F*) Number of platform site crossings during the probe test. (*G*) LXRβ KO mice exhibited disturbed reversal task of the Morris water maze test ($n = 11$ WT, 10 LXRβ KO, $^{*}P < 0.05$, two-way ANOVA, Bonferroni multiple comparison test). (*H*) Number of platform site crossings during the reversal probe test. (*I* and *K*) Representative heat maps showing the total time and location of during the 10-min social approach task (*I*) and social novelty recognition (*K*). Warmer colors (red) indicate greater time the mice spend exploring. (*J* and *L*) Quantification of the results in *I* and *K*, as shown by the amount of time spent in the chamber ($n = 10$ WT, 11 LXRβ KO; $^{*}P < 0.05$, $^{**}P < 0.01$, one-way ANOVA). Data are expressed as mean ± SEM in all panels.

KO mice have marked deficits in social function. We then assayed repetitive behaviors, which are thought to be ASD-like, by measuring self-grooming. LXRβ KO mice spent more time grooming themselves than did their WT littermates (Fig. 6*C*). Thus, LXRβ ablation could cause ASD-like behaviors in mice.

Discussion

Here, we have demonstrated that LXRβ was dynamically expressed during DG development and that mutation of LXRβ led to DG hypoplasia, highlighting its importance in DG neurogenesis and hippocampus-dependent functions. We determined that LXRβ was involved in the formation of the HF and transhilar radial glial scaffold in the developing DG, which might direct NPC migration to DG and SGZ. We also observed that LXRβ affected secondary RGC development during DG development, thereby determining the number of RGCs involved in adult neurogenesis and partly interfering with maturation of granule neurons, both with respect to morphology and function. We have demonstrated that LXRβ could control the ability of the DG to maintain long-term neurogenic capacity, and this information provides an important framework for understanding why LXRβ KO mice have ASD-like perturbations.

LXRβ was expressed specifically in nuclei of cells in the developing DG from the DG primordium and dentate migration stream to SGZ. The transhilar radial glial scaffold, by directing progenitor cells to the formation of SPZ, is a key player in the development of DG (8, 33). Aberrations in this scaffold in LXRβ KO were evident from reduced Nestin$^+$ and BLBP$^+$ processes present in the hilus. The area of the SPZ, outlined with GFAP staining, was diminished in LXRβ KO mice, suggesting that LXRβ deletion likely impairs migration of progenitor cells necessary for formation of the SPZ. Such a defect was further confirmed by BrdU birth-dating experiments. Thus, a retardation in migration toward to DG might explain hypoplasia in the DG with decreased Tbr2$^+$ IPCs and Sox2$^+$ NPCs in the mutant DG at P2.

Normally, the amorphous hilus, filled with mixed newly born neurons and precursors, undergoes a conversion into a highly radially organized structure during the first postnatal week (34). This reorganization is apparently important for the continuing generation and proper distribution of granule cells. There were fewer BrdU-positive cells labeled at P2 in the GCL of LXRβ KO than in WT DGs, and this was accompanied by an increased number of BrdU-positive cells in the hilus. There appears to be a migration deficit of dentate precursors to the GCL from the hilus along the transhilar radial glial scaffold. We also observed that there were fewer Sox2$^+$ NPCs and Tbr2$^+$ IPCs located in the SGZ of mice at P7 in LXRβ KO mice and that some cells were redistributed to the GCL. Thus, LXRβ ablation also impairs NPC migration from the GCL to the SGZ.

The GCL develops in a radial, outside-in gradient pattern, which requires a glia-guided migration step (35). The secondary radial glial scaffold initially develops in the first postnatal week, whose processes traverse the forming GCL and guide neuronal migration (21, 22). We have demonstrated that the secondary radial glial scaffold was diminished in the SGZ by loss of LXRβ. Such a decrease would lead to the observed improper distribution of dentate progenitors and granule cells. There is an involvement of canonical Notch1 signaling in the development and maintenance of RGC in the DG (25). Indeed, NPCs in the postnatal and adult SGZ are derived from secondary RGCs in the forming DG (21, 22). The present study found that deletion of LXRβ in mice decreased the expressions of Notch1 and its downstream effectors Hes1 and BLBP, which might explain its reduction of the secondary RGCs during early postnatal DG development. Further studies confirming the direct interaction between Notch1 and LXRβ are needed.

Previous reports have demonstrated that the LXRβ is critical for the development of dopaminergic neurons in the ventral midbrain (36, 37). Here, we revealed that there was a decrease in the number of CB and Prox1-expressing dentate granule neurons in postnatal LXRβ KO mice. Decreased DG neurogenesis has been further confirmed in adult LXRβ KO mice. It may be inferred that the LXRβ is also required for cell type-specific differentiation of dentate granule cells. The long unbranched processes of RGCs have been implicated in conveying signals that reflect the state of the local environment, thereby instructing the neurons to promote dendritic outgrowth (38). We have previously demonstrated that Bergmann glia directed dendrite development of Purkinje cells (14). In the present study, we observed that LXRβ deletion typically damaged RGCs in the GCL at P14, and this damage may result in impaired hippocampal spinogenesis and decreased level of synaptophysin.

There is evidence that defects in neurogenesis are associated with ASD both in humans (39) and in mouse models of ASD (3, 4, 40). The behavioral studies confirmed that ablation of LXRβ caused behavior disorders relevant to major ASD symptoms. Social interaction deficits, as key phenotypic traits of ASD, were evident in LXRβ KO mice. Increased repetitive behavior, also a hallmark of ASD, was increased in LXRβ KO mice. LXRβ KO mice were also found to display impairment in reversal learning, modeling resistance to change in routine, and insistence on sameness or rigid habits observed in ASD patients.

Our findings suggest early changes in DG neurogenesis and neuronal specification and/or localization that ultimately provide an aberrant template upon which to build the circuitry that is involved in normal social function. This biological mechanism, however, sheds light on both how DG development is regulated but also on the molecular events that lead to autism-like behavior in the LXRβ KO mouse.

Materials and Methods

The generation of LXRβ KO mice has been previously described (41). LXRβ KO heterozygotes were intercrossed and inspected at 9:00 AM on the following day for the presence of vaginal plugs. Noon of this day was assumed to correspond to E0.5. Three-month-old male mice were used for all behavioral experiments and adult neurogenesis, and embryonic and postnatal mice younger than 2 wk, both male and female mice, were used. All animals were housed in the Animal Facility of the Third Military Medical University in a controlled environment on a 12-h light/12-h dark illumination schedule and were fed a standard pellet diet with water provided ad libitum. All experimental procedures were performed in accordance with approved principles of laboratory animal care and ethical approval by the Third Military Medical University. Details of methods related to immunohistochemical analyses and immunofluorescence, BrdU Labeling, Golgi staining, Western blot analysis, behavioral tests, imaging and quantification and statistical analysis are provided in *SI Appendix, SI Materials and Methods*.

ACKNOWLEDGMENTS. This study was supported by National Natural Science Foundation of China Grant 31571069, the Swedish Research Council, the Center for Innovative Medicine, the Novo Nordisk Foundation, and Robert A. Welch Foundation Grant E-0004 (to J.Å.G.).

1. Lazarov O, Hollands C (2016) Hippocampal neurogenesis: Learning to remember. *Prog Neurobiol* 138–140:1–18.
2. Zhao C, Deng W, Gage FH (2008) Mechanisms and functional implications of adult neurogenesis. *Cell* 132:645–660.
3. Currais A, Farrokhi C, Dargusch R, Goujon-Svrzic M, Maher P (2016) Dietary glycemic index modulates the behavioral and biochemical abnormalities associated with autism spectrum disorder. *Mol Psychiatry* 21:426–436.
4. Li H, et al. (2014) Cell cycle-linked MeCP2 phosphorylation modulates adult neurogenesis involving the Notch signalling pathway. *Nat Commun* 5:5601.
5. Segal-Gavish H, et al. (2016) Mesenchymal stem cell transplantation promotes neurogenesis and ameliorates autism related behaviors in BTBR mice. *Autism Res* 9:17–32.
6. Yu DX, Marchetto MC, Gage FH (2014) How to make a hippocampal dentate gyrus granule neuron. *Development* 141:2366–2375.
7. You L, et al. (2015) The lysine acetyltransferase activator Brpf1 governs dentate gyrus development through neural stem cells and progenitors. *PLoS Genet* 11:e1005034, and erratum (2015) 11:e1005329.
8. Barry G, et al. (2008) Specific glial populations regulate hippocampal morphogenesis. *J Neurosci* 28:12328–12340.

9. Xu L, Tang X, Wang Y, Xu H, Fan X (2015) Radial glia, the keystone of the development of the hippocampal dentate gyrus. *Mol Neurobiol* 51:131–141.
10. Jakobsson T, Treuter E, Gustafsson JÅ, Steffensen KR (2012) Liver X receptor biology and pharmacology: New pathways, challenges and opportunities. *Trends Pharmacol Sci* 33:394–404.
11. Whitney KD, et al. (2002) Regulation of cholesterol homeostasis by the liver X receptors in the central nervous system. *Mol Endocrinol* 16:1378–1385.
12. Fan X, Kim HJ, Bouton D, Warner M, Gustafsson JA (2008) Expression of liver X receptor beta is essential for formation of superficial cortical layers and migration of later-born neurons. *Proc Natl Acad Sci USA* 105:13445–13450.
13. Xing Y, Fan X, Ying D (2010) Liver X receptor agonist treatment promotes the migration of granule neurons during cerebellar development. *J Neurochem* 115: 1486–1494.
14. Yang Y, et al. (2014) Activation of liver X receptor is protective against ethanol-induced developmental impairment of Bergmann glia and Purkinje neurons in the mouse cerebellum. *Mol Neurobiol* 49:176–186.
15. Xu P, et al. (2014) Liver X receptor β is essential for the differentiation of radial glial cells to oligodendrocytes in the dorsal cortex. *Mol Psychiatry* 19:947–957.
16. Sugiyama T, Osumi N, Katsuyama Y (2013) The germinal matrices in the developing dentate gyrus are composed of neuronal progenitors at distinct differentiation stages. *Dev Dyn* 242:1442–1453.
17. Förster E, Zhao S, Frotscher M (2006) Laminating the hippocampus. *Nat Rev Neurosci* 7:259–267.
18. Hodge RD, et al. (2013) Tbr2 expression in Cajal-Retzius cells and intermediate neuronal progenitors is required for morphogenesis of the dentate gyrus. *J Neurosci* 33: 4165–4180.
19. Li G, Kataoka H, Coughlin SR, Pleasure SJ (2009) Identification of a transient subpial neurogenic zone in the developing dentate gyrus and its regulation by Cxcl12 and reelin signaling. *Development* 136:327–335.
20. Iwano T, Masuda A, Kiyonari H, Enomoto H, Matsuzaki F (2012) Prox1 postmitotically defines dentate gyrus cells by specifying granule cell identity over CA3 pyramidal cell fate in the hippocampus. *Development* 139:3051–3062.
21. Brunne B, et al. (2013) Role of the postnatal radial glial scaffold for the development of the dentate gyrus as revealed by Reelin signaling mutant mice. *Glia* 61:1347–1363.
22. Brunne B, et al. (2010) Origin, maturation, and astroglial transformation of secondary radial glial cells in the developing dentate gyrus. *Glia* 58:1553–1569.
23. Tian C, et al. (2012) Foxg1 has an essential role in postnatal development of the dentate gyrus. *J Neurosci* 32:2931–2949.
24. Breunig JJ, Silbereis J, Vaccarino FM, Sestan N, Rakic P (2007) Notch regulates cell fate and dendrite morphology of newborn neurons in the postnatal dentate gyrus. *Proc Natl Acad Sci USA* 104:20558–20563.
25. Sibbe M, Förster E, Basak O, Taylor V, Frotscher M (2009) Reelin and Notch1 cooperate in the development of the dentate gyrus. *J Neurosci* 29:8578–8585.
26. Choe Y, Kozlova A, Graf D, Pleasure SJ (2013) Bone morphogenic protein signaling is a major determinant of dentate development. *J Neurosci* 33:6766–6775.
27. Dumas TC, Powers EC, Tarapore PE, Sapolsky RM (2004) Overexpression of calbindin D(28k) in dentate gyrus granule cells alters mossy fiber presynaptic function and impairs hippocampal-dependent memory. *Hippocampus* 14:701–709.
28. Kwon SE, Chapman ER (2011) Synaptophysin regulates the kinetics of synaptic vesicle endocytosis in central neurons. *Neuron* 70:847–854.
29. Cohen SJ, et al. (2013) The rodent hippocampus is essential for nonspatial object memory. *Curr Biol* 23:1685–1690.
30. Rudy JW, Sutherland RJ (1989) The hippocampal formation is necessary for rats to learn and remember configural discriminations. *Behav Brain Res* 34:97–109.
31. Cohen NJ, Eichenbaum H (1991) The theory that wouldn't die: A critical look at the spatial mapping theory of hippocampal function. *Hippocampus* 1:265–268.
32. Kondratiuk I, et al. (2013) Glycogen synthase kinase-3beta affects size of dentate gyrus and species-typical behavioral tasks in transgenic and knockout mice. *Behav Brain Res* 248:46–50.
33. Hodge RD, et al. (2012) Tbr2 is essential for hippocampal lineage progression from neural stem cells to intermediate progenitors and neurons. *J Neurosci* 32:6275–6287.
34. Eckenhoff MF, Rakic P (1984) Radial organization of the hippocampal dentate gyrus: A Golgi, ultrastructural, and immunocytochemical analysis in the developing rhesus monkey. *J Comp Neurol* 223:1–21.
35. Edwards MA, Yamamoto M, Caviness VS, Jr (1990) Organization of radial glia and related cells in the developing murine CNS. An analysis based upon a new monoclonal antibody marker. *Neuroscience* 36:121–144.
36. Theofilopoulos S, et al. (2013) Brain endogenous liver X receptor ligands selectively promote midbrain neurogenesis. *Nat Chem Biol* 9:126–133.
37. Sacchetti P, et al. (2009) Liver X receptors and oxysterols promote ventral midbrain neurogenesis in vivo and in human embryonic stem cells. *Cell Stem Cell* 5:409–419.
38. Sommer L, Rao M (2002) Neural stem cells and regulation of cell number. *Prog Neurobiol* 66:1–18.
39. Wegiel J, et al. (2010) The neuropathology of autism: Defects of neurogenesis and neuronal migration, and dysplastic changes. *Acta Neuropathol* 119:755–770.
40. Stephenson DT, et al. (2011) Histopathologic characterization of the BTBR mouse model of autistic-like behavior reveals selective changes in neurodevelopmental proteins and adult hippocampal neurogenesis. *Mol Autism* 2:7.
41. Alberti S, et al. (2001) Hepatic cholesterol metabolism and resistance to dietary cholesterol in LXRbeta-deficient mice. *J Clin Invest* 107:565–573.